

N O T I C E

THIS DOCUMENT HAS BEEN REPRODUCED FROM
MICROFICHE. ALTHOUGH IT IS RECOGNIZED THAT
CERTAIN PORTIONS ARE ILLEGIBLE, IT IS BEING RELEASED
IN THE INTEREST OF MAKING AVAILABLE AS MUCH
INFORMATION AS POSSIBLE

NASA Technical Memorandum 81512

(NASA-TM-81512) DEVELOPMENT OF
IMPROVED-DURABILITY PLASMA SPRAYED CERAMIC
COATINGS FOR GAS TURBINE ENGINES (NASA)
25 p HC A02/MF A01

CSSL 21E

N80-23313

Unclas
20304

63/07

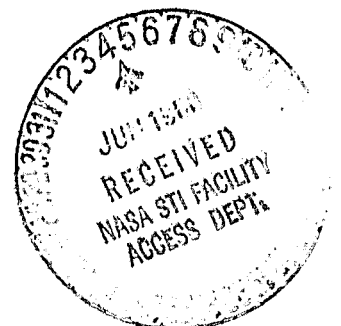
DEVELOPMENT OF IMPROVED-DURABILITY
PLASMA SPRAYED CERAMIC COATINGS
FOR GAS TURBINE ENGINES

Irving E. Sumner
Lewis Research Center
Cleveland, Ohio

and

Duane L. Ruckle
Pratt and Whitney Aircraft
East Hartford, Connecticut

Prepared for the
Sixteenth Joint Propulsion Conference
cosponsored by the AIAA, ASME, and SAE
Hartford, Connecticut, June 30-July 2, 1980



DEVELOPMENT OF IMPROVED-DURABILITY PLASMA SPRAYED CERAMIC COATINGS FOR GAS TURBINE ENGINES

Irving E. Sumner*
NASA Lewis Research Center
Cleveland, Ohio

and

Duane L. Ruckle**
Pratt and Whitney Aircraft
East Hartford, Connecticut

Abstract

As part of a NASA program to reduce fuel consumption of current commercial aircraft engines, Pratt and Whitney Aircraft is conducting an investigation to improve the durability of plasma sprayed ceramic coatings for use on vane platforms in the JT9D turbofan engine. Increased durability concepts under evaluation include use of improved strain tolerant microstructures and control of the substrate temperature during coating application. Initial burner rig tests conducted at temperatures to 1010° C (1850° F) indicated that improvements in cyclic life greater than 20:1 over previous ceramic coating systems were achieved. Three plasma sprayed coating systems applied to first stage vane platforms in the high pressure turbine were subjected to a 1000-cycle JT9D engine endurance test with only minor damage occurring to the coatings.

Introduction

The need for increased fuel efficiency in current and future gas turbine aircraft engines has been emphasized by recent shortages in the production of petroleum products and the subsequent price increases. The National Aeronautics and Space Administration (NASA) has initiated fuel conservation programs to alleviate the effect of the energy shortage on the aviation industry.¹ One such program is the Engine Component Improvement (ECI) Program managed by the Lewis Research Center. The Performance Improvement (PI) effort within the ECI Program is specifically directed at providing technological advances to improve the near term fuel efficiency of current turbofan engines.²

One of the PI concepts funded by NASA is an investigation currently being conducted by Pratt and Whitney Aircraft (P&WA) to demonstrate the use of plasma sprayed ceramic thermal barrier coatings in the JT9D-70/59 turbofan engine. The specific application is for the first stage vane platforms in the high pressure turbine. In this application, a thermal barrier coating in conjunction with a redesigned vane platform cooling system would allow for a reduction in the cooling air requirements.³ The fabrication costs of the first stage vanes could also be reduced by elimination of the film cooling holes in the platform. Use of this concept is anticipated to result in a reduction of 0.2 percent in the

specific fuel consumption and provide a payback period of zero time. Additional reductions in specific fuel consumption could be realized when coatings of sufficient durability for use on vane airfoils and turbine blades become available.

Approach

The durability limitations of plasma sprayed (PS) ceramic coatings applied to metallic engine components are due, in part, to the wide differences in the coefficient of thermal expansion of the metallic and ceramic materials.⁴ This results in significant strain mismatches between the metallic substrate and the ceramic coating that may cause the coating to spall. Figure 1 shows the ranges of strain mismatch that would be expected at both room temperature and a temperature condition of 1010° C (1850° F) as a function of the substrate temperature achieved when the ceramic coating was applied. For the nominal PS parameters and the burner rig bars used in the durability tests in this investigation, for example, the substrate temperature would approach approximately 425° C (800° F) during the application of the PS coating. Therefore, a compressive strain in the plane of the coating would be imposed on the coating when the test specimen was cooled to room temperature. Similarly, a somewhat larger tensile strain would be imposed on the coating when the test specimen was heated to the normal test temperature of 1010° C (1850° F).

The objective of this investigation was the development of a series of advanced PS ceramic coatings based on the concept of improved strain tolerance.³ Strain tolerance may be improved through control of the coating structure by (1) reducing the occurrence of damaging flaws and (2) providing desired discontinuities within the coating. Damaging flaws in the plane of the coating may result from the layer like buildup during the PS operation and may lead to the propagation of cracks and eventual spallation. Discontinuities within the coating may be provided in the form of increased porosity, random internal microcracking, or segmentation (through thickness cracking). These discontinuities would tend to reduce the modulus of elasticity of the coating structure, thereby reducing the local stresses. One additional concept of improving strain tolerance was through control of the substrate temperature during the application of the coating. This would provide a better balance between compressive and tensile strains imposed on the coating at both the low and high temperatures of the normal operating range.

The PI ceramic thermal barrier coating (TBC) program involves an iterative overall approach to

*Project Engineer, Engine Component Improvement Office.

**Assistant Project Metallurgist, Materials Engineering and Research Laboratory.

(1) refine the application and other process parameters of PS ceramic coatings to achieve the desired microstructure and optimize the strain mismatch, (2) determine the coating durability through burner rig testing under controlled laboratory test conditions, and finally (3) determine coating durability under actual JT9D engine operating conditions in 1000-cycle engine endurance tests. This paper summarizes the more significant results from the tasks just mentioned for the first iteration, including the first engine test. Other elements of the PI TBC program which will not be discussed in this paper include a two-dimensional strain analysis of the ceramic coating and a redesigned vane platform cooling system to take advantage of the presence of the TBC.

Plasma Sprayed Coating Parameters

Several plasma sprayed coating parameters were varied to develop an optimum set of spray conditions to reduce the occurrence of damaging flaws, and also to provide the desired porosity, microcracking or segmentation of the coating. The PS parameters varied included the coating chemistry, gun to specimen distance, powder particle size, and powder feed rate (Table I). Of these parameters, the variation in powder feed rate did not result in any apparent differences in coating microstructure, and a feed rate of 35 gm/min (1.2 oz/min) was selected for all coating systems. Initially, the temperature of the substrate was not controlled during the PS application process. Later in the investigation, control of the substrate temperature over a range from -35° to 650° C (-35° to 1200° F) was used to determine the effect of this parameter on coating durability. For this investigation, the baseline PS ceramic coating was a 20 percent by weight (w/o) yttria stabilized zirconia (YSZ) coating having the nominal spray parameters noted in Table I.

The variations in PS parameters for the TBC systems selected for presentation in this paper are shown in Table II. The variations in powder particle size, coating chemistry and specimen to gun distance provided the improved strain tolerance characteristics of porosity, microcracking and segmentation as noted. Laser scanning of the surface of a PS ceramic coating provided another technique of creating a segmented coating while controlling the temperature of the substrate provided a means of optimizing the strain mismatches between the coating and the metallic substrate. An electron beam/physical vapor deposited (EB/PVD) coating was also included in the test program to compare its durability with that of the PS coatings. The EB/PVD coating was finely segmented and may represent a near optimum segmented structure. A brief description of each coating will be given in the Discussion of Burner Rig Test Results section which follows.

The powders used for each PS coating were consistent throughout this investigation. In general, composite powders having spherical particles were used for the coarse 20 w/o YSZ coating while partially fused/sintered and crushed powders were used for the other coatings. The variation in particle size distributions are shown in Table III. The primary difference between the coarse and fine powders was the increased percentage of particles in the -120 to +230 mesh range for the coarse powder.

Plasma Sprayed Coating Application

The PS ceramic coatings tested in the burner rig were applied to 1.27 cm (0.50 in.) diameter bars approximately 10 cm (4 in.) long cast from Mar-M 509 cobalt base alloy. All burner rig bars were solid with the exception of those used for the controlled substrate temperature specimens which were hollow to allow cooling of the bar during application of the coating. All of the TBC systems tested were a two layer system consisting of a Ni-22Co-18Cr-13Al-0.7Y bond coating 0.08 to 0.13 mm (3 to 5 mil) thick and a ceramic coating 0.25 mm (10 mil) thick. The bars were grit blasted to roughen the surface and then coated using automated PS application equipment. The bars were rotated at 600 rpm while the Plasmadyne SG100 gun was traversed along the bar at a speed of 91 cm/min (36 in/min). Standard spray parameters were used, including a power input of 800 amps and 50 volts, an 85% argon/15% helium arc gas mixture, a powder feed rate of 35 gm/min (1.2 oz/min), and a 7.6 cm (3 in.) gun to specimen distance, except as noted. Three specimens for each coating system were prepared for burner rig testing. Coated specimens were exposed to a 1080° C (1975° F) heat treatment in a hydrogen atmosphere for 4 hours with the exception of the MSZ specimens which were tested without any heat treatment.

Burner Rig Durability Tests

Burner rig tests were performed to determine the relative durability of the various TBC systems in a cyclic thermal environment. Twelve of the TBC test specimens mounted in a test fixture and ready for burner rig testing are shown in Fig. 2. The thermal cycle consisted of a 4 minute period of heating to a maximum temperature of 1010° C (1850° F) followed by a 2 minute period of cooling to approximately 260° C (500° F) or less. The test fixture was rotated at 1725 rpm in the exhaust gas stream of a Jet A fueled burner to provide a relatively uniform hot temperature environment for all test specimens (Fig. 3). The gas velocity at the specimen location was Mach 0.3. The specimen temperature was monitored and controlled using an optical pyrometer and an automatic feedback controller to vary the fuel flow to the burner. The emittance of the test specimens was measured periodically, and corrections were applied to maintain accurate test temperatures. During the cooling period of the cycle, the burner was automatically moved away from the test fixture and forced air cooling was directed at the test specimens.

Testing was discontinued after periods of approximately 20 hours (200 cycles) to allow for visual examination of the specimens with a low power (X10) microscope. Specimen failure was considered to have occurred when the coating had spalled from 50 percent or more of the "test" zone of the burner rig bar. Such a failure typically occurred as a massive spall noted during a single inspection. The test zone was an area approximately 2.5 cm (1 in.) in length at the center of the exposed portion of the bar which experienced the maximum 1010° C (1850° F) temperature level during the thermal cycle.

Three specimens of each PS coating were tested while four EB/PVD specimens were tested.

In general, the burner rig test results indicated a wide range of coating durability. The durability, expressed as the average number of thermal cycles to failure of those specimens tested, is shown in Fig. 4. The baseline TBC system survived for an average of only 210 cycles before failure occurred. This baseline coating system, in general, was representative of the state-of-the-art ceramic coatings of approximately 1977. In contrast to the baseline, the TBC system with increased porosity survived for approximately 6000 cycles before the coating spalled, an improvement in durability of nearly 30:1. The microcracked 21 w/o MSZ and segmented 20 w/o YSZ (2.5 cm (1 in.) gun to specimen distance) coating systems provided an improvement in durability of greater than 20:1 (5200 and 5500 cycles, respectively). Two of the three test specimens for the segmented 6 w/o YSZ coating also exhibited relatively long life (4410 and 5040 cycles) while the third specimen failed after a very short time (1570 cycles) which reduced the average cycles to failure to 3670. However, the coatings that exhibited the best durability were the EB/PVD coating and the PS coatings applied with controlled substrate temperatures of 20° and 315° C (70° and 600° F). The durability of the EB/PVD coating was 10 420 cycles while the durability of these controlled substrate temperature coatings was 9400 and 9260 cycles, respectively. This was an improvement of greater than 40:1 over the baseline coating. On the other end of the scale, the segmented laser scanned coating and the 650° C (1200° F) substrate coatings performed the poorest, surviving only 220 and 130 cycles, respectively.

Discussion of Burner Rig Test Results

Baseline TBC

The baseline 20 w/o YSZ PS coating applied using the -325 mesh fine powder was a relatively dense coating having a porosity of approximately 10 percent. The coating had a fully stabilized cubic structure with only a very small amount of the monoclinic phase as determined by X-ray diffraction analyses. This was typical of all of the 20 w/o YSZ coating systems. A comparison of the microstructures representative of the pre-test and post-test condition of the coating is shown in Fig. 5. The very dense structure of the ceramic coating most likely resulted in relatively high stresses within the coating. It was observed that the coatings normally failed by exhibiting buckling of the ceramic during the cold portion of the thermal cycle. This appeared to be caused by compressive stresses in the plane of the coating and the resultant tensile stress normal to the plane of the coating. These stresses would tend to create cracks in the plane of the coating such as shown in Fig. 5(b).

Increased Porosity TBC

This 20 w/o YSZ TBC was applied using a coarser -170 mesh powder. The resulting coating was less dense than the baseline, having a porosity of approximately 15-20 percent. A comparison of the microstructures of the coating representative of the pre-test and post-test conditions is shown in Fig. 6. The durability of this coating (6000 cycles) was due to the strain tolerance provided by the porous microstructure which effec-

tively reduced the modulus of elasticity from that of a more dense structure. Some limited microcracking of the ceramic microstructure can also be seen, both before and after testing. The microcracks lying in the plane of the coating (parallel to the ceramic/bond coat interface) might be expected to propagate and eventually lead to spallation of the coating.

A typical burner rig bar coating failure is shown in Fig. 7. The ceramic coating spalled adjacent to the ceramic/bond coating interface leaving a thin irregular layer of ceramic still attached to the bond coating. This failure is consistent with the cracks seen in the microstructure (Figs. 5 and 6) and also with previous findings which indicated that the region of the coating immediately adjacent to the bond coating was the weakest link in the structure.⁵

Microcracked TBC

An increased level of microcracking in the ceramic structure was obtained by varying the baseline chemistry from 20 w/o YSZ to 21 w/o MSZ. All other plasma spray parameters remained the same. The microstructure for this coating is shown in Fig. 8. The 21 w/o MSZ coating has a partially stabilized cubic structure which may undergo a phase transformation to a tetragonal structure with a considerable fraction of the monoclinic phase. Some free magnesium oxide (MgO) particles may also be found. Both the monoclinic ZrO₂ and the free MgO contribute to the extensive microcracking in the coating. The microcracking was essentially discontinuous and random in direction. These microcracks, in general, did not tend to propagate, although the start of two larger cracks, one normal to and one in the plane of the coating, could be noted after testing (Fig. 8(b)). The crack in the plane of the coating could ultimately lead to a failure of the coating. For this coating system, the microcracking apparently acted as an effective strain relief mechanism as evidenced by the 5230 cycle durability determined in the burner rig test.

Segmented TBC

Segmentation of a ceramic coating can be defined as a series of fine cracks normal to the coating/substrate interface that extend through the coating to the bond coat. A segmented ceramic coating would then exhibit a columnar structure. The presence of the fine cracks would be expected to provide a mechanism for accommodating mismatch strains created by the different rates of expansion between the metallic substrate and the ceramic coating.

One technique of creating a segmented ceramic coating was to reduce the baseline gun to specimen distance from 7.6 to 2.5 cm (3 to 1 in.). The microstructure of the porous 20 w/o YSZ PS coating using the reduced gun distance is shown in Fig. 9. For this case, the coating exhibited an increased density due to melting which resulted from the extreme heat. Upon cooling, segmentation cracks were created normal to the plane of the coating. Some cracking (or increased porosity) also occurred parallel to the plane of the coating (Fig. 9(a)) which would have an adverse effect on

coating durability. These cracks tended to propagate into larger cracks, such as can be noted in Fig. 9(b), during the burner rig testing. The durability of this coating (5490 cycles) indicated that the segmented structure did relieve the strain mismatches. However, additional investigation and careful control of the PS application parameters would be required to optimize this system by eliminating the flaws in the plane of the coating while still maintaining the desired segmentation characteristics.

A second technique of creating a PS segmented ceramic structure was the 6 w/o YSZ coating where a fine particle size powder (~325 mesh) had been used (Fig. 10). The 6 w/o YSZ was only partially stabilized and underwent a partial transformation from a cubic to a tetragonal phase upon cooling. The segmentation was believed to be due to a volume reduction associated with the phase transformation, thereby creating tensile stresses which resulted in cracking of the coating normal to the interface. Two of the test specimens exhibited a relatively long life (4410 and 5040 cycles) while the third specimen failed at 1570 cycles. However, the 6 w/o YSZ was considered to be one of the more promising systems tested. For this particular segmented coating, the characteristic size of a typical segmented column was about 1 mm (40 mil). The remnant segmentation pattern remaining on the burner rig bar after testing was completed is shown in Fig. 11. Further investigation is required, particularly to develop a more porous microstructure using a coarser particle size powder as used in some previous investigations.⁶

The third technique of providing a segmented PS coating was to scan the surface of the baseline 20 w/o YSZ coating with a laser beam. The intense heat produced by the laser beam melted and densified the ceramic coating. Upon cooling, residual segmentation cracks normal to the plane of the coating were produced. The laser scanning was performed using a CO₂ laser with a wavelength of 10.6 microns. The laser beam was focused to produce either a circular or an elliptical "donut" shaped beam. Two examples of the microstructures produced during preliminary tests on flat 5 cm (2 in.) square test coupons for varying laser beam conditions are shown in Fig. 12. In each case, cracking of the ceramic coating normal to the interface and extending just to the bond coat was achieved.

Laser scanning of round burner rig bar specimens was accomplished with a 8.8 cm (3.45 in.) elliptical beam, a power input of 5 kW and a scanning speed of approximately 1.27 cm/sec (30 in./min). However, it was necessary to use the porous 20 w/o YSZ coating system and to preheat the coated round bar specimens to 845° C (1550° F) prior to the laser scanning process to avoid premature spallation of the coating upon cooling after laser scanning was completed. The preheating apparently allowed accommodation of thermal strains induced in the coating by the intense laser heating. Looking back to the preliminary tests using the flat coupons, these same thermal strains had apparently been accommodated by actual bending of the thin metal substrate.

The laser scanned segmented coatings survived an average of only 220 cycles in the burner rig test. Subsequent metallographic examination of the pre-test structure indicated that the laser

scanning had not produced cracking which extended completely through the ceramic to the bond coat. This allowed additional cracks to develop through the porous inner structure parallel to the plane of the coating causing spalling. The critical nature of the laser scanning process indicated that additional work would be required to make this segmentation technique acceptable.

The last technique employed to achieve a segmented coating was to apply a 20 w/o YSZ coating with an electron beam/physical vapor deposition (EB/PVD) process. This technique required the use of a vacuum chamber and was relatively complex compared to the PS technique. However, the EB/PVD process produced a coating with a finely segmented structure consisting of long, thin columns (Fig. 13). This columnar structure probably represented a near optimum size and spacing for a segmented coating. The durability of the EB/PVD coating (10 420 cycles) in the burner rig tests confirmed that the EB/PVD coating was very strain tolerant. The post-test examination of the failed coating (Fig. 14) revealed that internal oxidation of the bond coating had occurred. This led to debonding of the bond coating from the Mar-M 509 substrate. Therefore, the performance of the bond coating precluded an evaluation of the full potential durability of the EB/PVD coating.

Temperature Controlled Substrate TBC

For all of the PS ceramic coatings described up to this point, the temperature of the substrate was not controlled during application of the coatings. For the baseline gun to specimen distance of 7.6 cm (3 in.), the temperature of the burner rig bars was estimated to approach approximately 425° C (800° F) during coating application. A relatively high compressive stress would then be imposed on the coating parallel to the interface while a tensile stress normal to the interface would be created as the bar cooled to room temperature. These stresses would tend to form cracks parallel to the plane of the coating causing spallation, as noted earlier for the baseline TBC. A reduction of the compressive strain in the plane of the coating, and therefore increased spalling resistance, would be expected to result from a decrease in the substrate temperature during the coating application.

To determine whether changes in the residual stresses would significantly affect coating durability, a number of hollow burner rig bars were coated with the porous 20 w/o YSZ coating system while maintaining various controlled substrate temperatures. Temperatures of -35°, 20° (room temperature) and 315° C (-35°, 70° and 600° F) were maintained by controlling a flow of liquid nitrogen or room temperature air through the hollow bars. A temperature of 650° C (1200° F) was maintained by using a natural gas burner to heat the bars. Temperatures of the bars were monitored with thermocouples embedded in the walls.

The most durable PS coatings were those applied with the substrate temperature controlled at 20° or 315° C (70° or 600° F). These coatings survived approximately 9300 to 9400 cycles before failure, thereby performing almost as well as the EB/PVD coating. Again, however, thermal mismatch strains were not the only factor

contributing to spalling of the ceramic coating. Two other factors were: (1) oxidation of the bond coating, and (2) bending of the burner rig bars during the testing. Oxidation of the bond coating (Fig. 15) resulted in a volume expansion, which effectively forced spallation of the ceramic coating. The bending of the burner rig bars (Fig. 16) was caused by oxidation of the Mar-M 509 substrate in the internal cooling passage which weakened the bar. The centrifugal force from the rotation of the test fixture caused the bar to bend, thereby applying additional stresses to the ceramic material. For these reasons, the full potential durability of these coatings also was not achieved.

Engine Test

Three PS ceramic coatings were selected for the first JT9D-70 engine test: (1) porous 20 w/o YSZ coating, (2) microcracked 21 w/o MSZ coating, and (3) segmented 6 w/o YSZ coating. Information obtained for the three PS ceramic coatings was expected to provide a baseline against which the validity of the burner rig tests and the durability of the thermal barrier coatings subjected to the second engine test could be measured. The controlled substrate temperature coating process was not chosen because the equipment required to control the vane platform temperature was not yet available. The EB/PVD coating was not chosen because of (1) the durability demonstrated with the PS coatings, and (2) the relatively higher complexity and cost of applying the ceramic coating to the vane platform configuration.

The platforms on a total of 18 test vanes were hand plasma sprayed with coatings as follows: 6 vanes - 20 w/o YSZ, 7 vanes - 21 w/o MSZ, and 5 vanes - 6 w/o YSZ. The coating thickness was 0.38 mm (15 mil).

The cooling scheme for the vane platforms was redesigned to take advantage of the insulating effect of the ceramic coating. The normal film cooling holes were replaced by an impingement cooling system installed on the back side of the vane platforms. The cooling air flow for this engine test was reduced approximately 50 percent from that used for the film cooling concept. The spent cooling air was exhausted through the vane platform trailing edge. The design criteria for the cooling system was that the average metal temperature of the coated vane platforms should be equivalent to the B/M vane platforms.

The test vanes were instrumented with a number of thermocouples to measure cooling air and platform metal temperatures. Pressure sensors were also used to measure the pressure drop across the impingement plates.

The engine test conducted was a 1000 cycle endurance test. The basic test cycle consisted of operation at flight idle, simulated full reverse, ground idle, and takeoff power levels. A series of intermediate power levels were also run every 100 cycles. The total time at takeoff and simulated full reverse power levels was more than 80 hours.

Preliminary data obtained during the engine test at the takeoff power level indicated that the vane platform metal temperatures were more uniform

(i.e., less severe thermal gradients along the platform) for the thermal barrier coated vanes than for the B/M vanes. Also, the average metal temperatures of the coated platforms were found to be significantly less than that for the B/M vane platforms.

Preliminary inspection of the test vanes after removal from the engine indicated that they had been subjected to a severe 1000 cycle endurance test in terms of the turbine inlet temperature. Of the 36 platforms coated with a ceramic TBC, nine platforms exhibited some slight to moderate spallation of the coating, as can be noted in Fig. 17. However, most of these vanes had been clustered together in a very hot region of the circumferential temperature profile of the combustor. The remaining 27 platform coatings survived the engine test with no apparent damage.

Concluding Remarks

The durability of plasma sprayed ceramic coatings subjected to a cyclic thermal environment has been improved substantially by improving the strain tolerance of the ceramic structure and also by controlling the substrate temperature during the application of the coating. Improved strain tolerance was achieved by using ceramic structures with increased porosity, microcracking or segmentation. Plasma spraying on a controlled temperature substrate also has been shown to improve durability by reducing harmful residual stresses. Three strain tolerant ceramic coatings survived a 1000 cycle JT9D-70 engine endurance test with no apparent damage to 75 percent of the platform coatings; many of those coatings that spalled were located in a region of very high turbine inlet temperature.

This program is continuing with a second iteration of burner rig tests and another engine test, concentrating primarily on refining the substrate temperature control process for plasma sprayed coatings.

References

1. Nored, D. L., "Fuel Conservative Aircraft Engine Technology," Proceedings of the Eleventh Congress of the International Council of the Aeronautical Sciences, Vol. 1, International Council of the Aeronautical Sciences Secretariat (DGLR), Cologne, 1978, pp. 11-26. (Also NASA TM-78962, 1978).
2. McAulay, J. E., "Engine Component Improvement Program - Performance Improvement," AIAA Paper 80-0223, Jan. 1980. (Also NASA TM-79304, 1979).
3. Gaffin, W. O. and Webb, D. E., "JT8D and JT9D Jet Engine Performance Improvement Program - Task I: Feasibility Analysis," Pratt and Whitney Aircraft Group, East Hartford, Conn., PWA-5518-38, Apr. 1979. (NASA CR-159449).
4. Sevcik, W. R. and Stoner, B. L., "An Analytical Study of Thermal Barrier Coated First Stage Blades in a JT9D Engine," Pratt and Whitney Aircraft Group, East Hartford, Conn., PWA-5590, Jan. 1978. (NASA CR-135360).

5. Levine, S. R., "Adhesive/Cohesive Strength of a $ZrO_2 = 12$ w/o Y_2O_3 /NiCrAlY Thermal Barrier Coating," NASA TN-73792, 1978.
6. Stecura, S., "Effects of Compositional changes on the Performance of a Thermal barrier Coating System," Presented at the American Ceramic Society Third Annual Conference on Composite and Advanced Materials, Merritt Island, Florida, January 21-26, 1979. (Also NASA TN-78976, 1978).

TABLE I. - PLASMA SPRAY COATING PARAMETERS INVESTIGATED

Parameter	Range investigated	Baseline value
Chemistry	6-20 w/o YSZ ^a 21 w/o MSZ ^b 5 w/o CSZ ^c	20 w/o YSZ
Gun to specimen distance	2.5 - 15 cm	7.6 cm
Powder particle size	-325 mesh (fine) -170 mesh (coarse)	-325 mesh
Powder feed rate	10-40 gm/min	35 gm/min
Substrate temperature	Uncontrolled Controlled (-350 to 650° C)	Uncontrolled

^aYttria stabilized zirconia (Y_2O_3/ZrO_2).

^bMagnesium oxide stabilized zirconia (MgO/ZrO_2).

^cCalcium oxide stabilized zirconia (CaO/ZrO_2).

TABLE II. - SIGNIFICANT THERMAL BARRIER COATING SYSTEMS
SUBJECTED TO BURNER RIG TESTS

TBC systems	Change from baseline coating	Improved strain tolerance characteristics
20 w/o YSZ	Baseline	
20 w/o YSZ	Coarse powder	Porosity
21 w/o MSZ	Coating chemistry	Microcracking
20 w/o YSZ	2.5 cm gun to specimen distance, coarse powder	Segmentation
6 w/o YSZ	Coating chemistry	Segmentation
20 w/o YSZ	Surface laser scanned, coarse powder	Segmentation
20 w/o YSZ	EB/PVD coating	Segmentation
20 w/o YSZ	Controlled substrate temperature, coarse powder	Strain mismatch

TABLE III. - POWDER PARTICLE SIZE DISTRIBUTION USED FOR THERMAL
BARRIER COATING SYSTEMS

Coating chemistry	Powder	Particle distribution (percent) in given size range (mesh)				
		-170 to +120	-120 to +230	-230 to +270	-270 to +325	-325
20 YSZ	Coarse	0.8%	40.5%	2.8%	15.6%	40.3%
20 YSZ	Fine	0	0	0	0	100
6 YSZ	Fine	0.2	3.2	2.5	11.8	82.3
21 MSZ	Fine	0	1.7	3.2	24	71.1

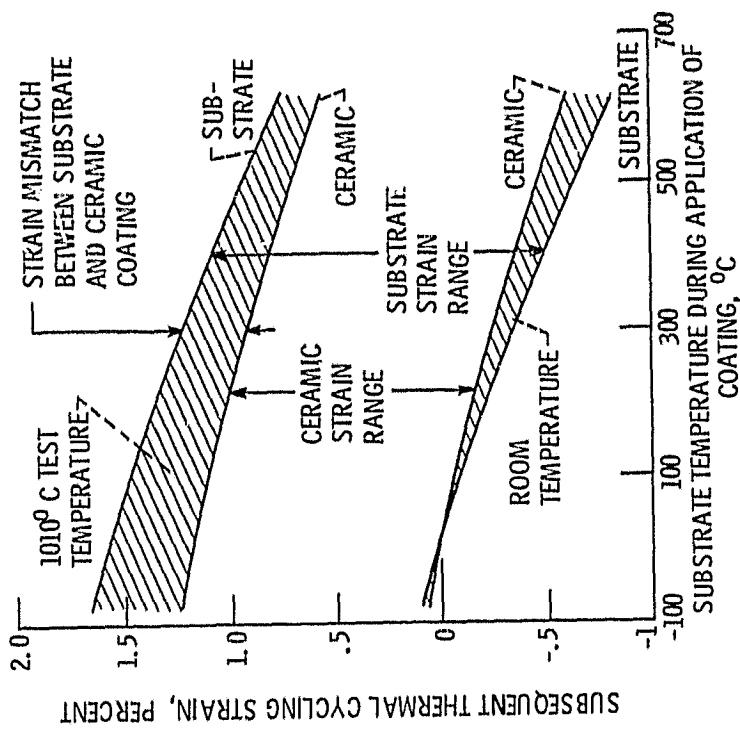


Figure 1. - Variation of interface strain mismatch with substrate temperature during application of thermal barrier coating (one dimensional analysis).

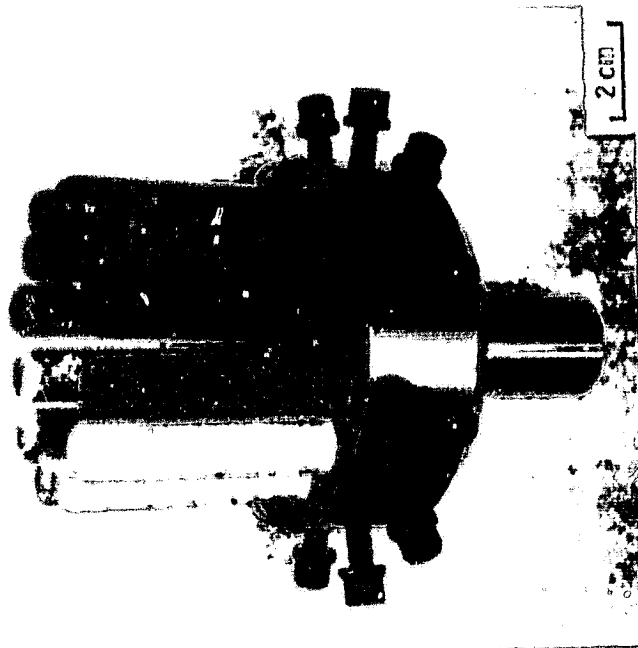


Figure 2. - TBC specimens in test fixture ready for burner rig testing.

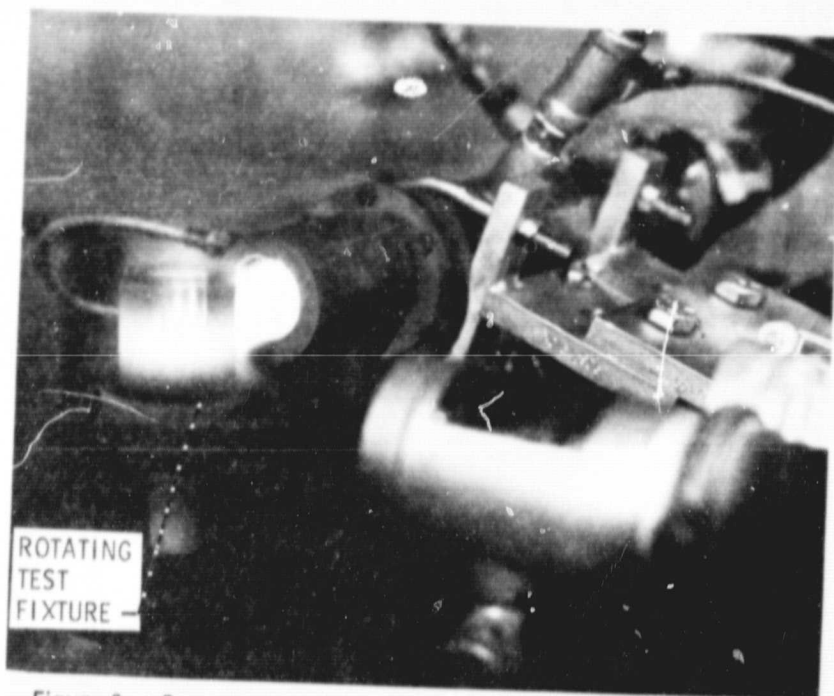


Figure 3. - Burner rig in operation during hot portion of the thermal cycle.

ORIGINAL PAGE IS
OF POOR QUALITY

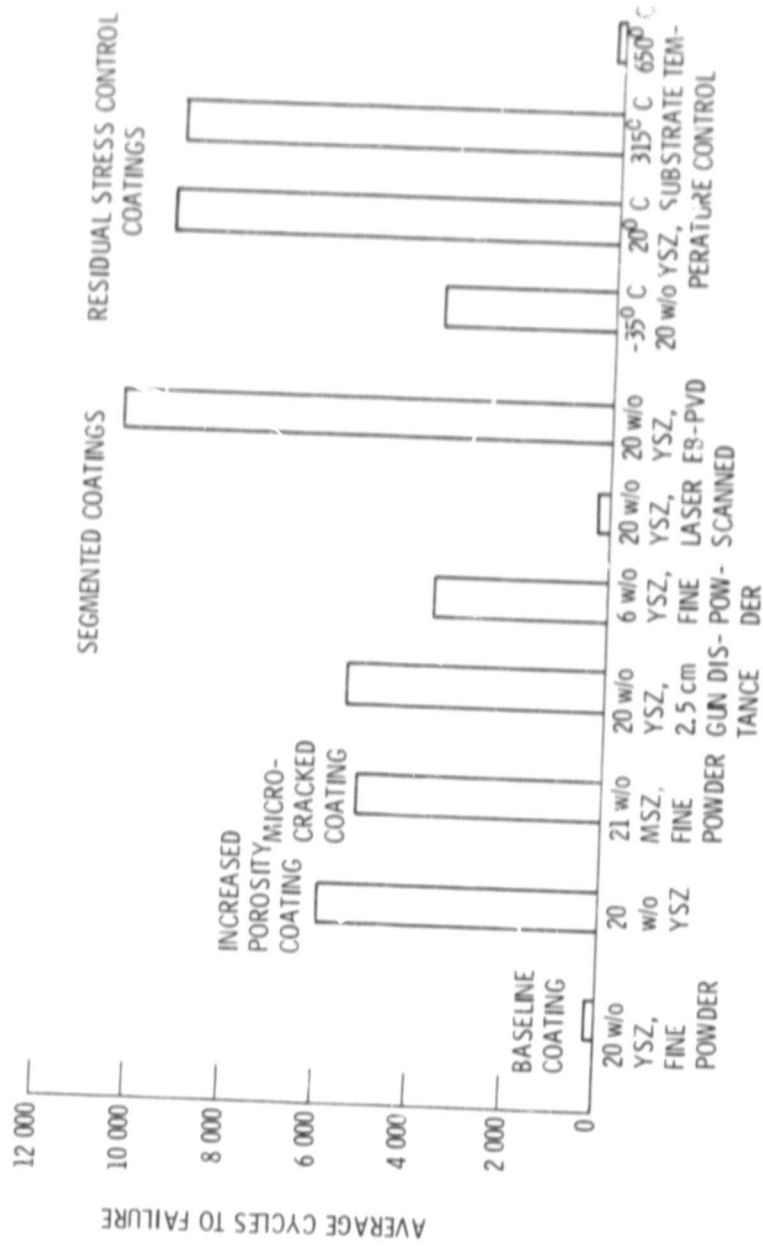
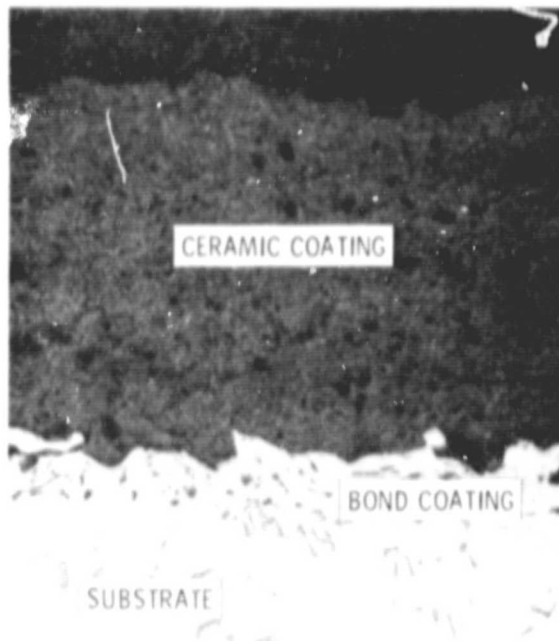
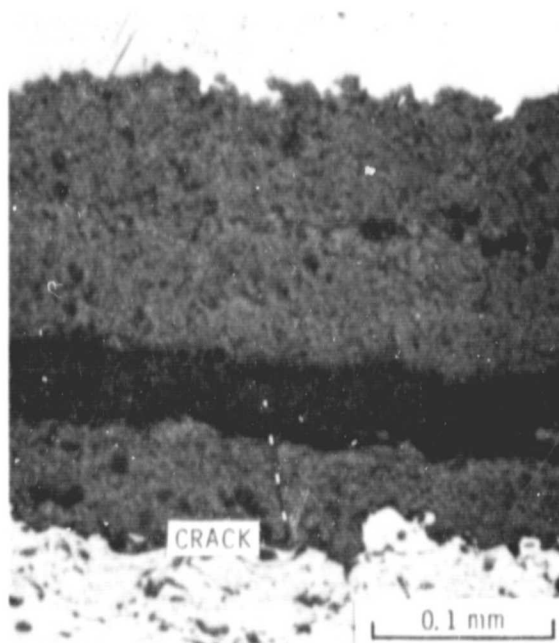


Figure 4. - Average number of thermal cycles to failure for several thermal barrier coating systems.



(a) PRE-TEST.

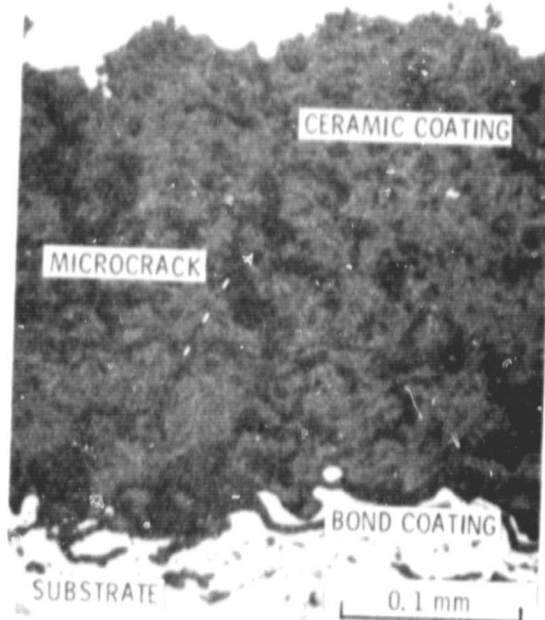


(b) POST-TEST.

Figure 5. - Dense microstructure of baseline 20 w/o YSZ TBC.



(a) PRE-TEST.



(b) POST-TEST.

Figure 6. - Porous microstructure of 20 w/o YSZ TBC using coarse (-170 mesh) powder.

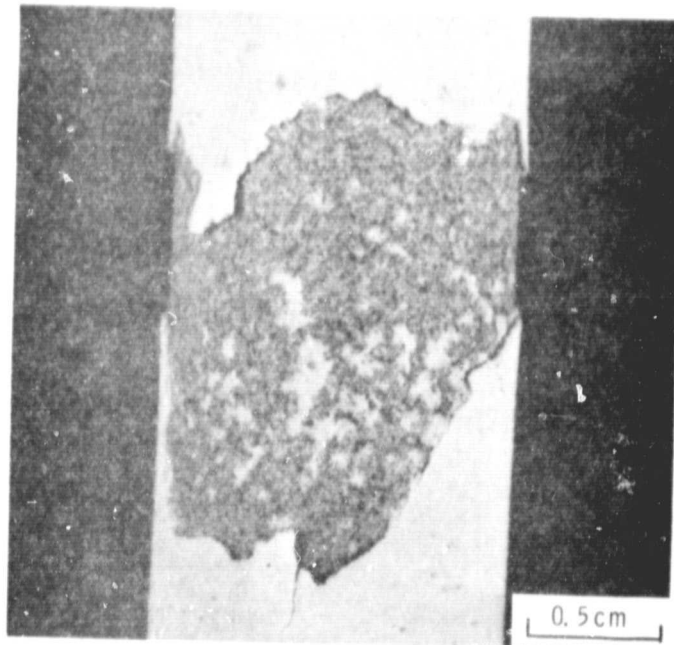
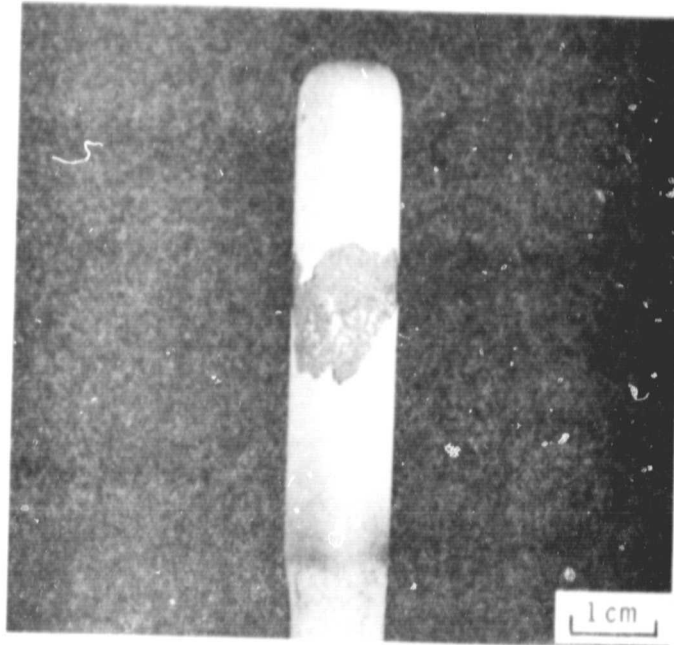
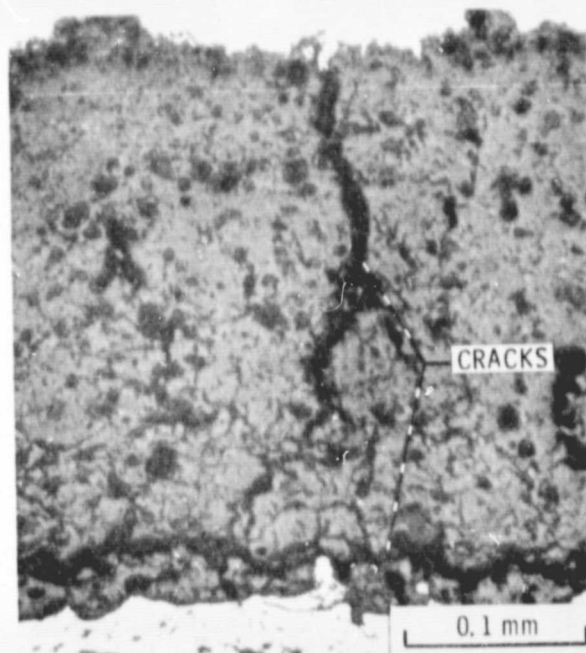


Figure 7. - Typical spallation failure of porous 20 w/o YSZ TBC after thermal cycling in burner rig test.

ORIGINAL PAGE IS
OF HIGH QUALITY

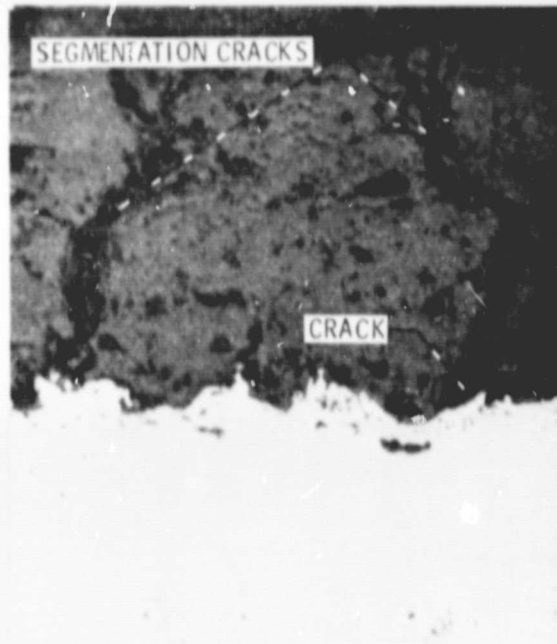


(a) PRE-TEST.

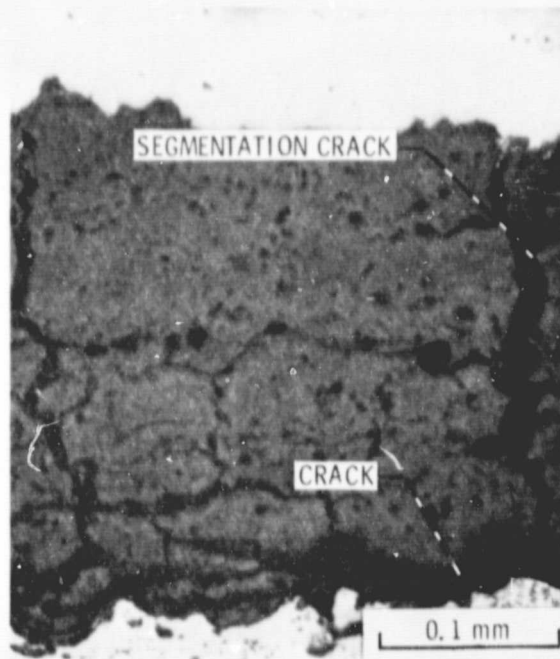


(b) POST-TEST.

Figure 8. - Microcracked microstructures of 21 w/o MSZ TBC.

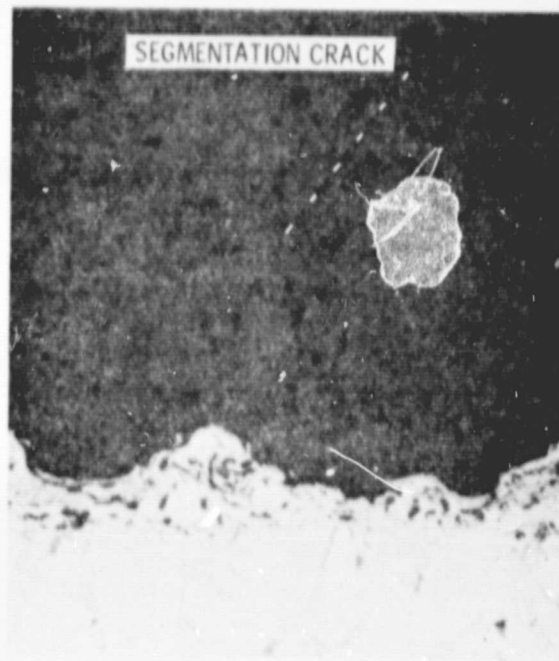


(a) PRE-TEST.



(b) POST-TEST.

Figure 9. - Segmented microstructures of 20 w/o YSZ TBC with 2.5 cm gun to specimen distance.



(a) PRE-TEST.



(b) POST-TEST.

Figure 10. - Segmented microstructures of 6 w/o YSZ TBC with fine powder.

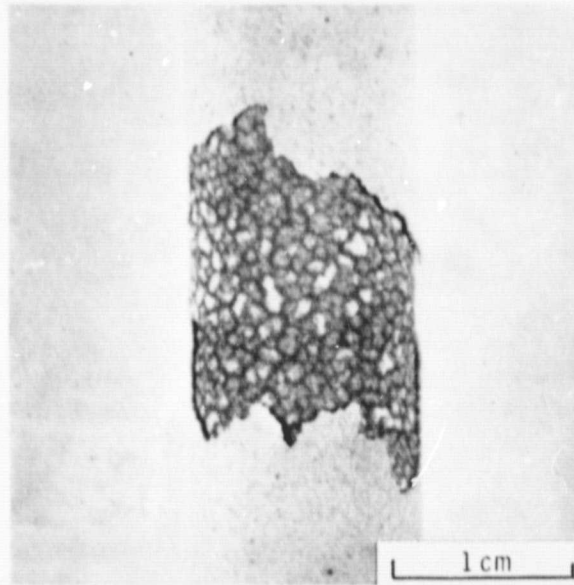
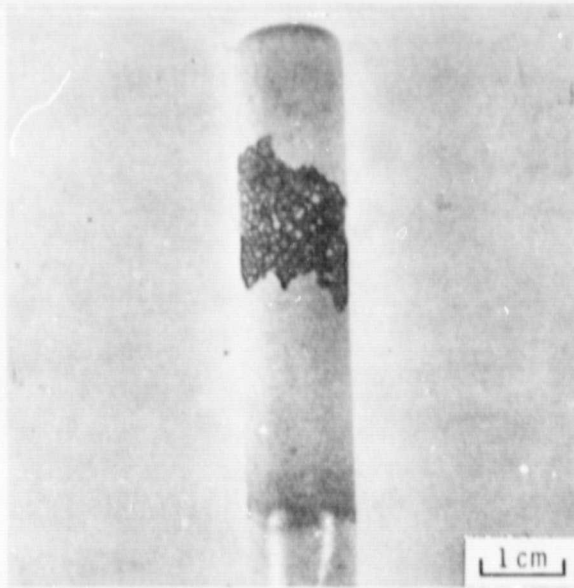
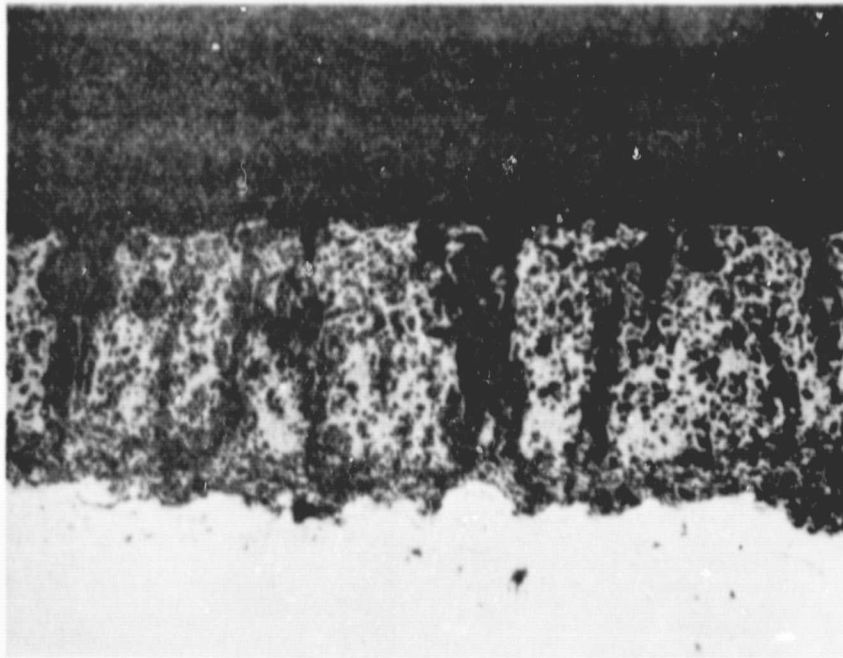
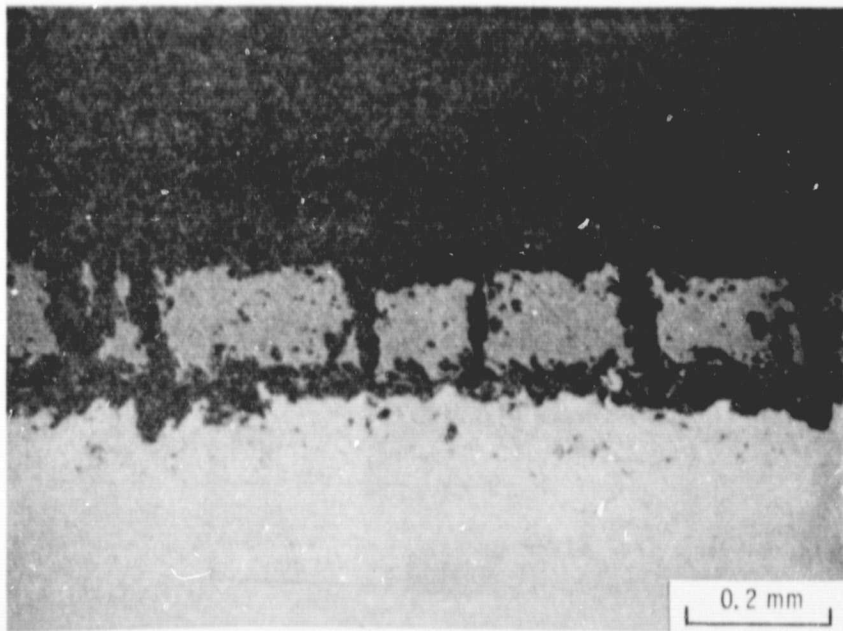


Figure 11. - Failure of 6 w/o YSZ TBC showing remnants of segmentation pattern in spalled region.



(a) 0.6 cm DIAMETER LASER BEAM PATTERN; 2 kW POWER INPUT; 4.2 cm/sec SCANNING SPEED.



(b) 6.1 cm ELLIPTICAL LASER BEAM PATTERN; 5 kW POWER INPUT; 2.1 cm/sec SCANNING SPEED.

Figure 12. - Segmented microstructures of 20 YSZ TBC using laser scanning.

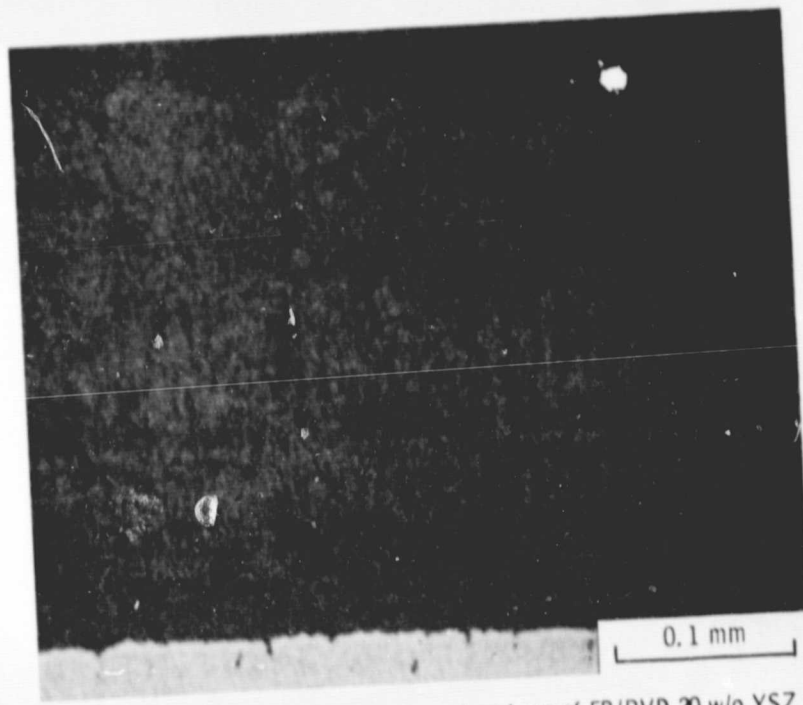
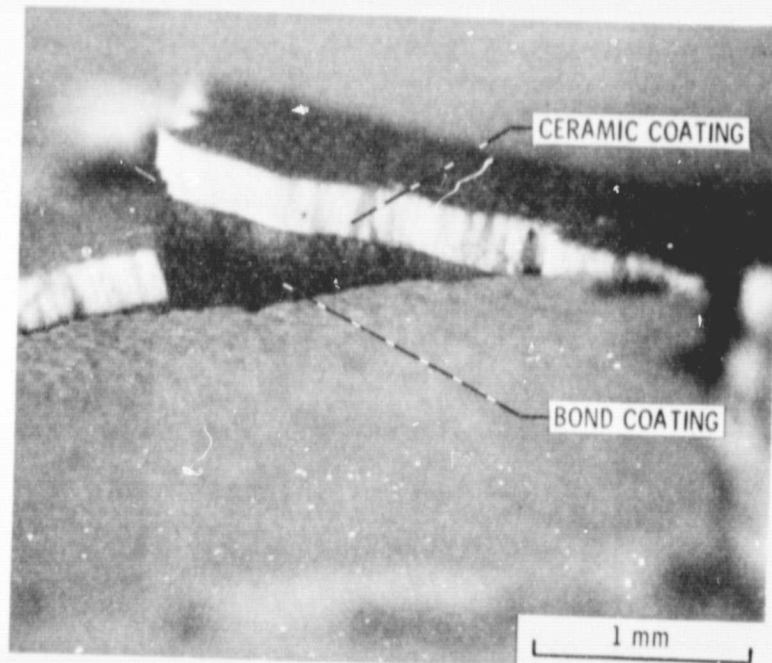


Figure 13. - Finely segmented microstructure of EB/PVD 20 w/o YSZ TBC.

ORIGINAL PAGE IS
OF POOR QUALITY

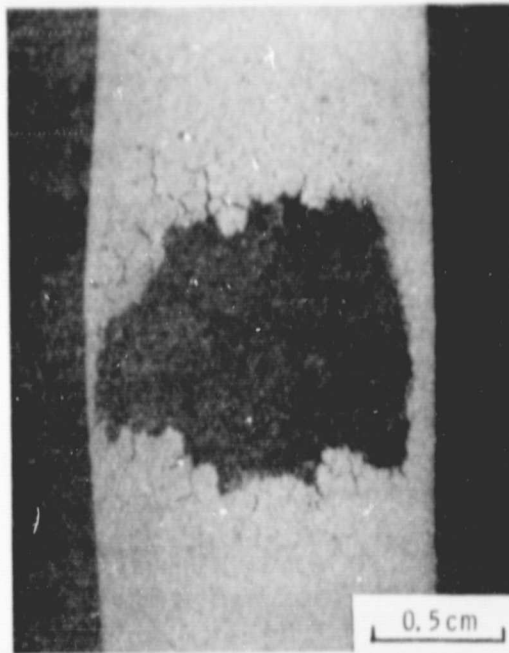


(a) FAILED REGION ON BURNER RIG BAR.

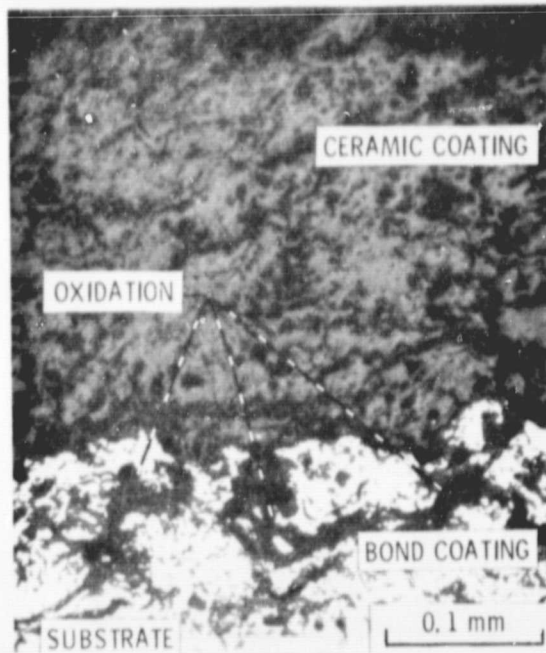


(b) CROSS-SECTION OF COATING SYSTEM FAILURE.

Figure 14. - Failure of MCrAlY bond coating for EB/PVD 20 w/o YSZ TBC specimen.

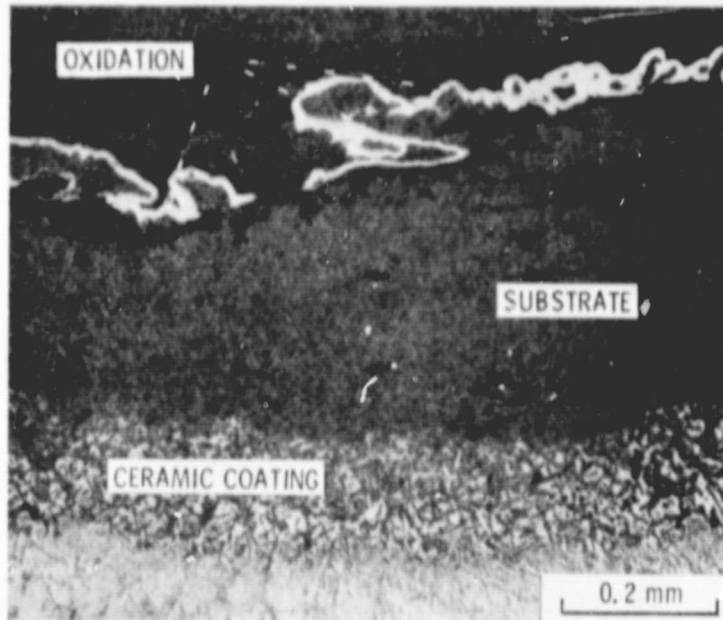


(a) SPALLED REGION OF BURNER RIG BAR.

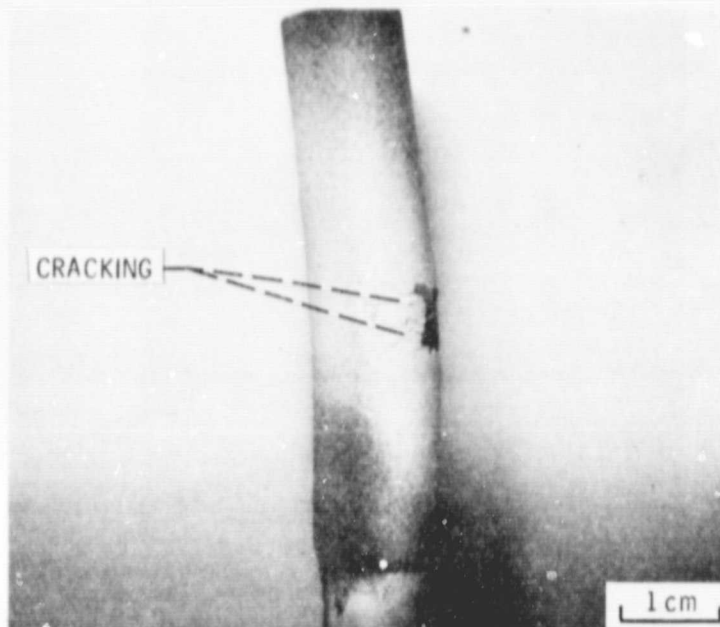


(b) MICROSTRUCTURE OF COATING SHOWING OXIDATION OF BOND COATING.

Figure 15. - Coating failure of 20 w/o YSZ TBC specimen with controlled 20⁰ C temperature substrate due to oxidation of bond coating.

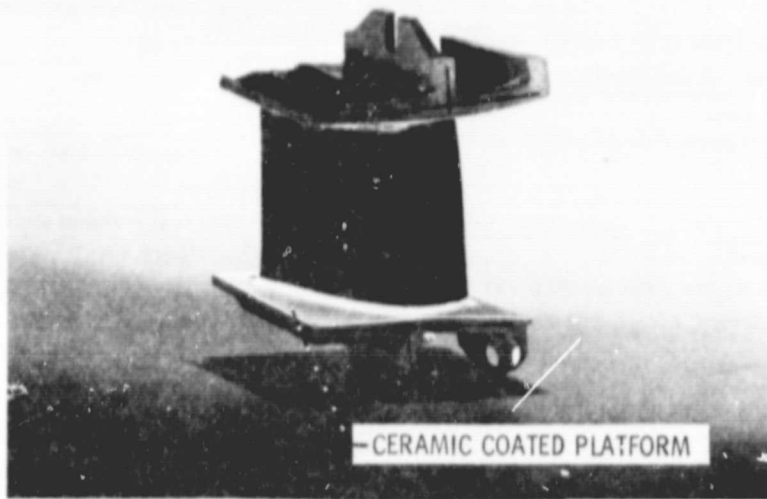


(a) INTERNAL OXIDATION.

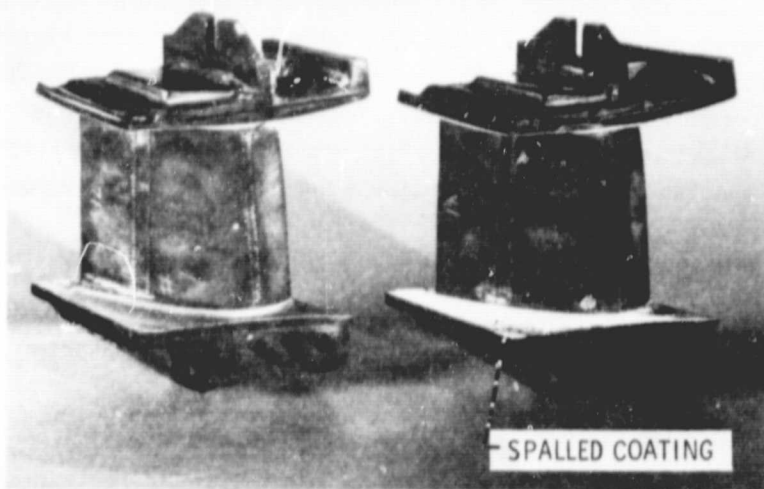


(b) BENDING OF BURNER RIG BAR AND RESULTANT CRACKING OF CERAMIC COATING.

Figure 16. - Coating failure of 20 w/o YSZ TBC specimens with controlled 20⁰ C temperature substrate due to internal oxidation and bending of burner rig bar.



(a) PRE-TEST CONDITION.



(b) POST-TEST CONDITION SHOWING COATING THAT SURVIVED INTACT (ON LEFT) AND COATING THAT SPALLED (ON RIGHT).

Figure 17. - First stage vanes with thermal barrier ceramic coatings used in engine test.